

<https://helda.helsinki.fi>

Nonequilibrium Liquid Liquid Phase Separation of Poly(N-isopropylacrylamide) in Water/Methanol Mixtures

Xue, Na

2017-06-13

Xue , N , Qiu , X-P , Aseyev , V & Winnik , F M 2017 , ' Nonequilibrium Liquid Liquid Phase Separation of Poly(N-isopropylacrylamide) in Water/Methanol Mixtures ' , Macromolecules , vol. 50 , no. 11 , pp. 4446-4453 . <https://doi.org/10.1021/acs.macromol.7b00407>

<http://hdl.handle.net/10138/308091>

<https://doi.org/10.1021/acs.macromol.7b00407>

cc_by_nc

acceptedVersion

Downloaded from Helda, University of Helsinki institutional repository.

This is an electronic reprint of the original article.

This reprint may differ from the original in pagination and typographic detail.

Please cite the original version.

Non-equilibrium Liquid-Liquid Phase Separation of poly(*N*- isopropylacrylamide) in Water/Methanol Mixtures

Na Xue[†], Xing-Ping Qiu[†], Vladimir Aseyev^{‡,⊥}, and Françoise M. Winnik^{*,†,‡,⊥}

[†]Department of Chemistry, University of Montreal, CP6128 Succursale Centre Ville,
Montreal QC Canada H3C 3J7

[‡]World Premier International (WPI) Research Center Initiative, International Center for
Materials Nanoarchitectonics (MANA) and National Institute for Materials Science (NIMS),
1-1 Namiki, Tsukuba 305-0044, Japan

[⊥]Department of Chemistry, University of Helsinki, FI-00014 Helsinki, Finland

ABSTRACT: Visual observation of solutions of PNIPAM-45K (n-butyl- end groups, obtained by RAFT polymerization of NIPAM, M_n 44,500 g·mol⁻¹, 10.0 g·L⁻¹) in water/methanol mixtures revealed that mixtures of methanol volume fractions (ϕ_M) ranging from 0.250 to 0.600 undergo macroscopic liquid-liquid phase separation (MLLPS) at 21 °C. Compared to the nominal composition of mixtures as prepared, the dense liquid phase is enriched in PNIPAM and in water, as determined by quantitative ¹H NMR spectroscopy. MLLPS took place also in mixed methanol/water systems polymer concentration ≤ 10 g L⁻¹) with a PNIPAM-80K obtained by standard free radical polymerisation, albeit over a narrow composition range ($0.57 < \phi_M < 0.65$). However, mixed MeOH/water systems with

Commented [AV1]: I think this title is too general and does not present novelty of this manuscript. Maybe "Non-equilibrium LLPS..."

Commented [fW2R1]:

PNIPAM-Cl (Cl- end groups, M_n 44,500 g·mol⁻¹, 10.0 g L⁻¹) did not show MLLPS. Observation by fluorescence microscopy of a mixed MeOH/water sample containing PNIPAM-45 K and a pyrene-labeled PNIPAM indicated that the surface of the dense phase droplets is enriched in PNIPAM, which is believed to affect the resistance of the droplets against coalescence. Mixed PNIPAM-45K/methanol/water) prepared and stabilized at 21 °C were either heated to 45.5 °C ($0.14 < \phi_M < 0.62$) or cooled to -40 °C ($0.25 < \phi_M < 0.50$) in order to obtain a temperature/composition map of the system. An interesting feature of the liquid-liquid phase separation reported here, both liquid phases remain cloudy or opaque for experimentally undefined long time, independently of their history both upon heating and cooling, which is a sign of metastability. The equilibrium state of lowest free energy that corresponds to two transparent phases, is never attained

Commented [AV3]: I would add here or somewhere that these droplets are a result of unstable microscopic liquid-liquid phase separation.

Commented [AV4]: An interesting feature of the studied liquid-liquid phase separation (both upon heating and cooling) is that in the final stage both liquid phases remain cloudy or opaque for experimentally undefined long time, which is a sign of metastability. We never reach equilibrium state with the lowest free energy that corresponds to two transparent phases.

Commented [fW5R4]:

INTRODUCTION

Solutions of poly(*N*-isopropylacrylamide) (PNIPAM) in pure water exhibit a heat-induced phase transition around a clouding temperature, $T_{CP} \sim 32$ °C.¹ The turbidity is the microscopic expression of the rupture of strong polymer-water interactions and the formation of strong interactions between the dehydrated, hydrophobic polymer chains that associate into objects hundreds of nanometers in diameter, such as mesoglobules. Within the liquid-liquid equilibrium (LLE) thermodynamic framework, the emergence of turbidity is described as the separation into two liquid phases: one phase consists of nearly pure water, the other phase has a high polymer concentration and nearly no water. Polymer/solvent systems kept at their clouding temperature for sufficiently long time may macroscopically separate into two transparent liquid phases, which corresponds to the final equilibrium phase state corresponding to the absolute minimum of free energy. This has been observed in the case of

polymethylvinylether (PVME), a polymer of low glass temperature, which may form an “oil phase” in equilibrium with an aqueous phase. The formation of two macroscopically separated phases has not been reported in the case of dilute aqueous PNIPAM systems kept at or just above T_{CP} for long time, possibly due to the high T_g value of PNIPAM (REF to our first review) and viscoelastic effect (REF to Chi Wu <http://pubs.acs.org/doi/abs/10.1021/ma049556n>). One can speak about colloidal stability of PNIPAM mesoglobules formed above T_c . This state does not correspond to the absolute minimum of free energy, but the system remains in a local minimum of energy for infinitely long time. It is hard to define whether PNIPAM above T_{CP} is in a liquid- or solid-like state. (REF to our first review) Nonetheless, parameters derived for the LLE model are very useful to model the temperature induced shrinking/swelling characteristics of PNIPAM crosslinked gels.

The solubility of PNIPAM in water is affected by the addition of a third component, such as a water-miscible good solvent of PNIPAM. The phenomenon, known as co-nonsolvency, is observed visually by the clouding of a clear aqueous PNIPAM solution kept at room temperature upon addition of specific amounts of a liquid, such as methanol, ethanol, 1,4-dioxane, or tetrahydrofuran, within solvent-specific composition ranges.²⁻⁴ Originally, the co-nonsolvency of PNIPAM in water/methanol mixtures was interpreted within the standard Flory-Huggins (FH) theory.⁵ Recently, this theory was extended to take into consideration the association of the solvent molecules and the competitive association between the solvent molecules and the polymer chain.⁶ F. Tanaka *et al.* put forward a different model that combines the cooperative character of the hydration/dehydration of the PNIPAM chain⁷ and the concept of competitive water/polymer and methanol/polymer hydrogen bonds formation. Zhang and Wu, in contrast, suggested that the conformational transition is driven by changes of the quality of the solvent rather than local polymer/solvent interactions.⁸ They noted that

water/methanol complexes of different composition form in mixed methanol/water depending on the methanol volume fraction, such that the solvent quality passes from good-to-bad-to-good with increasing methanol fraction. This change of solvent quality triggers the coil-to-globule-to-coil re-entrant transition of the PNIPAM chain. Interest in PNIPAM co-nonsolvency was rekindled by recent publications of alternative explanations of the phenomenon.⁹⁻¹² The theoretical LLE framework has not been used to model PNIPAM/water/alkohol systems, but it is often applied to model the behavior of crosslinked PNIPAM hydrogels in water/alkohol systems.

Commented [AV6]: Model ?

Commented [AV7]: (gels??? Then a REF needed maybe?)

Interestingly, Tao *et al.*²² reported that, when maintained at room temperature for extended time periods, turbid samples of PNIPAM in water/methanol (concentration $150 \text{ g} \cdot \text{L}^{-1}$, molar mass $150,000 \text{ g} \cdot \text{mol}^{-1}$) undergo MLLPS within specific solvent composition boundaries. They presented a partial ternary phase diagram and fitted the experimental data within the Flory-Huggins formalism using three binary interaction parameter and one ternary interaction parameter. This report raises a number of questions of high relevance to the current interest in the co-nonsolvency of PNIPAM in water/alkohol mixtures: Is the macroscopic demixed state observed experimentally an equilibrium state? How is it affected by the molar mass and concentration of PNIPAM? Is the phenomenon sensitive to the structure of the end-groups for samples of low molar mass PNIPAM? Are demixed samples prepared at room temperature affected by changes in temperature? The study reported here addresses these issues based on observations and data recorded for ternary PNIPAM/water/methanol systems, for which the polymer concentration ($10 \text{ g} \cdot \text{L}^{-1}$) is lower than for the system studied by Tao *et al.* REF Several samples of PNIPAM with different end-groups were used. We determine the composition of the two liquid phases for several mixed systems formed at room temperature. Using optical and fluorescence microscopy, we monitor the demixing at 21°C of PNIPAM/water/methanol systems confined between two glass slides. Freshly prepared

Commented [AV8]: Freshly prepared PNIPAM/water/methanol mixtures are milky due to formation of micro phase separated droplets containing large fraction of PNIPAM.

PNIPAM/water/methanol mixtures are milky due to formation of micro phase separated droplets containing a large fraction of PNIPAM. The dynamics of the droplets in demixed samples depend sensitively on the solvent composition. Finally, we construct the phase diagram of the ternary system as a function of temperature from -40 °C to + 50 °C. Invariably, all demixed samples reach a final state where both liquid phases are opaque or cloudy. This state perseveres for indefinitely long time, suggesting that the state attained is quasi stable and has not reach the absolute minimum of free energy.

EXPERIMENTAL SECTION

Materials. The α,ω -di(*n*-butylpropionate)-poly(*N*-isopropylacrylamides) (PNIPAM-45K and PNIPAM-26K) and α,ω -di(2-chloroethyl propionate)-PNIPAM (PNIPAM-45K(Cl)) were synthesized and characterized as described previously.¹³ PNIPAM-80K was obtained by standard free radical polymerization of NIPAM in *t*-butyl alcohol initiated with AIBN.²³ The pyrene-labeled polymer PNIPAM-Py (M_n 104,000 g mol⁻¹) was prepared as described previously.²⁴ It carries randomly ~ 0.12 mol %Py. Water was deionized using a Millipore Milli-Q system. Analytical grade methanol, trimethylsilyl propionic acid, sodium salt (TMPS, 98%) and deuterium oxide (99.9%) were purchased from Sigma-Aldrich Chemicals.

Sample preparation. Stock solutions of PNIPAM in water (10.0 g·L⁻¹) and in methanol (10.0 g·L⁻¹) were prepared and kept at room temperature for 1 day in tightly capped vials. Mixed samples (usually ~ 2.0 mL) were prepared by mixing weighed aliquots of the two stock solutions in the desired ratios. They were placed in tightly sealed conical glass vials and kept at room temperature (21 °C) for 2 days prior to evaluation, unless stated otherwise.

Determination of the composition of the heavy and light liquid phases formed at room temperature. Mixed samples (~1.0 g) were prepared by mixing weighed aliquots of

stock solutions of PNIPAM-45K (10.0 g·L⁻¹) in water and in methanol. The methanol volume fraction in the mixtures ϕ_M was calculated according to the following equation:

$$\phi_M = \frac{m_{Me}/\rho_{Me}}{m_{Me}/\rho_{Me} + m_W/\rho_W} \quad (1)$$

where m_{Me} is the mass of the methanolic stock solution, ρ_{Me} is the density of methanol, m_W is the mass of the aqueous stock solution, and ρ_W is the density of water. The mixed samples were placed in conical vials and kept at room temperature for 2 days. The upper phase, named “light phase” in the following, was recovered by pipetting and diluted in D₂O containing a trace amount of TMPS used as standard. The bottom phase, named “heavy phase” in the following, was also dissolved in D₂O/TMPS. ¹H NMR spectra of the resulting solutions were recorded on a Bruker AV400 MHz NMR spectrometer. The area of the signals at $\delta = 0$ ppm ((CH₃)₃ of TMPS), $\delta = 1.16$ ppm (CH₃ of PNIPAM), $\delta = 3.36$ ppm (CH₃ of methanol), and $\delta = 4.80$ ppm (H₂O) (Figure S1) was measured and used to calculate the composition of the samples.

The polymer volume fraction in the dense phase ϕ_P^D was calculated by the following equation,

$$\phi_P^D = X \cdot D \cdot a / \rho_P \quad (2)$$

where X is the weight percent of polymer in the dense phase (obtained from the ¹H NMR data), ρ_P is the density of PNIPAM (1.07 g·mL⁻¹)²², a is the density correction parameter for the water/methanol mixtures to take into account the non-linearity of the total volume of methanol/water mixtures vs. the sum of the volumes of pure water and pure methanol used to prepare the mixture (values of a are shown in Table S2 together with a description of the calculations), and D is the density of the dense phase.

The methanol volume fraction ϕ_M^D in the dense phase was calculated using equation 3, where ϕ' is the ratio of the volume of methanol to the sum of the volumes of methanol and water obtained from the ^1H NMR results.

$$\phi_M^D = (1 - \phi_P^D) \cdot \phi' \quad (3)$$

In all calculations, corrections were made to take into account the non-linearity of the volume of mixed water/methanol solutions vs the sum of the volumes of the stock solutions (in pure water and pure methanol) used to prepare them.²⁵ (see SI)

Density measurements. A mixed polymer/water/methanol sample (methanol volume fraction 0.4) was placed in a volumetric flask ($V = 25$ mL or 10 mL). Once macroscopic liquid-liquid phase separation was achieved (about 2.5 days), the upper phase was removed carefully with a glass pipette. The mass of the remaining dense phase (m_P) was determined. *n*-Hexane was added in an amount necessary to fill the volumetric flask precisely to the marked line. The volume of the *n*-hexane added was recorded. The density of *n*-hexane was determined to be $0.67 \text{ g}\cdot\text{mL}^{-1}$ using a 25 mL volumetric flask. The density of the polymer dense phase, D , was calculated using equation 4, where m_H and m_P are, respectively, the mass of added *n*-hexane and the mass of the dense phase. The density of the dense phase was $0.814 \text{ g}\cdot\text{mL}^{-1}$ ($\pm 0.055 \text{ g}\cdot\text{mL}^{-1}$) in water/methanol mixtures with methanol volume fraction 0.4. We determined the density of the dense phase for one composition and assumed that it was the same within the MLLPS region studied.

$$D = \frac{m_P}{V - m_H / 0.67} \quad (4)$$

LLPS observation by optical microscopy. A known amount of a freshly-mixed water/methanol sample of either PNIPAM-45K or PNIPAM-80K ($10.0 \text{ g}\cdot\text{L}^{-1}$) was placed on

a clean glass slide. The liquid was covered with a small round glass slide and sealed with epoxy glue as described in detail elsewhere.²⁶ The solution spreads between the two glass slides and forms a circular area. The distance between the two glass slides was ~ 1 mm, as estimated from the solution volume and the spreading area of the spread solution. Samples were immediately placed on the microscope stage kept at 21 °C and viewed with an Axioskop 2 Carl Zeiss Microscope and the Image-Pro-Plus software. Images of the samples were taken at various times for up to 2 days. They were calibrated with a standard scale viewed under the same conditions. The size of 700 to 2000 droplets was measured manually in a calibrated image. The number-averaged radius of the droplets in a specimen at a given time was calculated.

Fluorescence microscopy observation of LLPS droplets. Stock solutions ($10.0 \text{ g} \cdot \text{L}^{-1}$) of PNIPAM-45K containing 5 wt% of PNIPAM-Py were prepared by dissolving the appropriate amounts of the polymers in water and in methanol. They were mixed at a ϕ_M 0.40 yielding a turbid sample which was placed immediately on a clean glass slide. The liquid was covered with a small round glass slide and sealed with epoxy glue, as described above. The sample was placed on the microscope stage ($T = 21$ °C) and viewed with Carl Zeiss Microscope equipped with a Peltier-cooled CCD camera as detector. For fluorescence images, samples were excited at 358 nm and detected at 421 nm

Temperature dependence of MLLPS. a. $T > 21$ °C. Water/methanol mixed samples of PNIPAM-45K ($10.0 \text{ g} \cdot \text{L}^{-1}$, methanol volume fractions ϕ_M : 0.140 (± 0.002), 0.200, 0.450, 0.500 and 0.620) were prepared in conical glass vials tightly capped, sealed with paraffin film, and kept for 2 days at room temperature. They were placed in an ethylene glycol/water bath and heated from 21 °C to 45.5 °C in ~ 5 °C increments. The samples were kept at each

temperature for 2 h and their appearance was recorded. Samples were cooled back to 21 °C in one step either immediately or after a 24 h incubation at 45.5 °C.

b. $T < 21$ °C. Water/methanol mixed samples of PNIPAM-45K ($10.0 \text{ g}\cdot\text{L}^{-1}$, ϕ_M : 0.252, 0.300, 0.360, 0.401, 0.450 and 0.500) were prepared as in part a. (above) and were placed in an ethylene glycol/water bath. They were cooled from 21 °C to -40 °C in ~ 5 °C steps. The samples were kept at each temperature for 1 h (and their appearance was recorded). Cooled samples brought back to 21 °C recovered their original appearance.

RESULTS AND DISCUSSION

Phase separation of ternary PNIPAM/water/methanol samples at constant temperature (21 °C)

This first section probes the MLLPS in mixed samples prepared at 21 °C and kept at this temperature throughout the study. Four PNIPAM samples were used. Their molecular characteristics of the polymers are listed in Table 1, together with the volume fraction of methanol, ϕ_M^{min} of the ternary PNIPAM/water/methanol mixture of minimum cloud point temperature, T_c^{min} . The turbidity diagrams of PNIPAM-26K, PNIPAM-45K and PNIPAM-80K, taken from data reported previously,¹³ are presented in Figure 1a.

Commented [AV9]: Figure 1 is missing

Table 1. Characteristics of the Polymers Used

Polymers	M_n ($\text{g}\cdot\text{mol}^{-1}$)	\bar{D}	ϕ_M^{min}	T_c^{min}	Turbidity domain at 21 °C ($1.0 \text{ g}\cdot\text{L}^{-1}$)
PNIPAM-26K	26,400 ^a	1.04 ^a	0.47	6.9	$0.240 < \phi_M < 0.550$

PNIPAM-45K	44,500 ^a	1.10 ^a	0.50	4.6	0.240 < φ_M < 0.590
PNIPAM-80K	77,900 ^a	1.28 ^a	0.53	-1.0	0.240 < φ_M < 0.610
PNIPAM-45K(CI)	44,500 ^a	1.10 ^a	—	—	—

a. M_n and \bar{D} (polydispersity index) were determined by GPC using DMF.¹³

Ternary mixtures (polymer concentration: 10.0 g·L⁻¹) within the turbidity domains of water/methanol solutions of PNIPAM-26K, PNIPAM-45K, and PNIPAM-80K (1.0 g·L⁻¹)²⁷ were prepared and kept at 21 °C.⁸ The mixtures were monitored visually over several days. Initially, the samples within the co-nonsolvency region are uniformly turbid, as seen in Figure 1b (t= 0) in the case of a PNIPAM-45K mixed sample ($\varphi_M = 0.450$). With time, a vertical gradient of turbidity can be detected. The layer on the top becomes translucent and almost transparent. After 3 days, droplets form on the bottom of the vial. The droplets grow with time. After 4 days, the upper liquid layer is colorless and slightly turbid, the drop on the bottom remains turbid. The drop remains turbid after 7 days and the upper layer is still slightly opaque. Moreover, the appearance of the sample does not change when kept quiescent at room temperature for several months. The demixing occurs much faster (< 2 days) when the mixtures are placed in conical flasks, rather than flat-bottomed vials. For most experiments reported below, demixed samples were prepared in conical flasks and kept for 2 days at room temperature prior to analysis, unless stated otherwise. The incubation period (2 days in conical flasks) was chosen, somewhat arbitrarily, in view of the facts that after this time period, the visual appearance of the samples did not change with time and that this length of time is sufficiently short to ensure that the composition of the samples does not change due to solvent evaporation. We assumed that after this time, mixed samples have

reached a metastable state, the demixed liquid phases remained turbid and the final equilibrium state with absolute minimum of free energy was not attained.

Figure 1 (a) Turbidity diagram of PNIPAM-26K (blue triangles), PNIPAM-45K (black squares), and PNIPAM-80K (red full circles) in methanol/water mixtures; the black and red stars indicate the low and high ϕ_M values corresponding to the MLLPS domains at 21 °C (shown by the thick black and red horizontal lines) for PNIPAM-45K and PNIPAM-80K; the vertical arrows point to the minima of the T_c vs ϕ_M curves (coordinates T_c^{\min} and ϕ_M^{\min} listed in Table 1); polymer concentration : 1.0 g.L⁻¹; data from reference 27); (b) Photographs of a PNIPAM-45K/methanol/water mixture ($\phi_M = 0.45$, polymer concentration: 10.0 g.L⁻¹) kept at room temperature for 7 days; the red oval surrounds a drop of dense liquid phase.

Commented [AV10]: Figure 1 is missing

At 21 °C, all the ternary PNIPAM-45K samples within the turbidity domain ($0.240 < \phi_M < 0.590$, boundaries highlighted by black stars in Figure 1a) undergo MLLPS. For PNIPAM-80K, MLLPS occurs only in samples within the $0.570 < \phi_M < 0.650$ composition range (indicated by the red stars in Figure 1a), which corresponds to a narrow window within the turbidity range for this polymer at 21 °C ($0.200 < \phi_M < 0.630$). This difference signals that the molar mass and/or the end-groups of PNIPAM are important factors in facilitating MLLPS. To test the end-group effect, we prepared mixed samples of PNIPAM-45K(Cl), a polymer which has exactly the same molar mass of the PNIPAM-45K but carries ethylchloride end groups. The PNIPAM-45K(Cl)/water/methanol mixtures exhibits co-nonsolvency. However, the turbid mixtures of this polymer (10.0 g.L⁻¹) in water/methanol did not undergo MLLPS at 21 °C. They remained uniformly turbid for several months. The role of end groups and polymer molar mass in MLLPS will be addressed again in light of experiments described below.

Composition of the dense and lean phases in ternary mixtures within the MLLPS region (21 °C). Ternary PNIPAM-45K (10.0 g.L⁻¹)/water/methanol samples (2.5 mL) were prepared and kept at room temperature for 2 days. The lean and dense phases were separated and analysed

by quantitative ^1H NMR spectroscopy in D_2O , as described in the Experimental section, Table S1, and Figure S1. The composition of the two phases, expressed in volume fractions, is given in Table 2 for 4 samples of different “nominal composition”, defined as the volume fraction of the three components calculated based on the weights of the methanol and water stock solutions used to prepare the sample. The table gives the volume fractions of methanol (ϕ_M), water (ϕ_W) and polymer (ϕ_P) in the initial mixtures and in the dense/lean phases of the demixed samples with corresponding superscripts. The methanol molar fraction (x_m) in the initial mixture is included since it is commonly used in the literature. The ternary phase diagram of PNIPAM-45K/water/methanol constructed with the values listed in Table 2 is shown in Figure S2. In all samples, the dense phase is enriched in polymer. The polymer concentration in the dense phase increases with increasing nominal methanol fraction up to 0.240 or $\sim 240 \text{ g}\cdot\text{L}^{-1}$. The lean phase contains much less polymer ($\sim 1 \text{ g}\cdot\text{L}^{-1}$). Moreover, the solvent in the heavy phase is enriched in water, whereas the light phase is enriched in methanol.

Table 2. Composition of the dense and lean phases in the phase separated samples and in the initial mixtures.

Nominal composition ^a				Composition of the demixed samples ^b					
				Dense phase			Lean phase		
ϕ_M	x_m	ϕ_W	ϕ_P	ϕ_M^D	ϕ_W^D	ϕ_P^D	ϕ_M^L	ϕ_W^L	ϕ_P^L
0.350	0.235	0.640	0.010	0.206	0.647	0.147	0.238	0.761	0.001
0.386	0.264	0.604	0.010	0.199	0.596	0.205	0.325	0.674	0.001
0.452	0.321	0.538	0.010	0.251	0.524	0.225	0.389	0.610	0.001

0.498 0.363 0.492 0.010 0.253 0.507 0.240 0.423 0.576 0.001

^a. Nominal composition of the mixtures upon mixing, calculated from the weight of the methanol and the water stock solutions used to prepare them; φ_M , φ_W , φ_P are the volume fractions of methanol, water, and polymer, respectively; x_m is the methanol molar fraction.

^b. Composition in the dense/lean phases in the demixed samples; the volume fractions of the components are defined the same way as in the initial mixtures. The number average standard error is $\sim 11\%$.

Next, we observed the phase separation process by optical microscopy. Aliquots of freshly prepared PNIPAM/water/methanol samples were transferred on a glass slide, sealed, mounted on the stage of an optical microscope kept at 21 °C, and observed immediately. Micrographs recorded during the demixing of the ternary system of $\varphi_M = 0.500$ are presented in Figure 2(a-d). Within 5 min after mixing, droplets appeared, coalesced, and grew in size reaching radii of $\sim 2.0 \mu\text{m}$ within 18 min (Figure 2a). After 8 h, the mixture consisted of a population of droplets of broad size distribution with an average radius of $\sim 2.9 \mu\text{m}$ (Figure 2c). The droplets continued to grow in size over the next 16 h, yielding a large number of elongated drops with protrusions consisting of linked small droplets. Microscopic observations of ternary systems of $\varphi_M = 0.247$, 0.600 were performed under the same conditions. For each sample the average droplet radius was determined experimentally at various times up to 24 h. Plots of the time evolution of droplets radii are presented in Figure 2e for the three samples. For the sample with $\varphi_M 0.600$, the droplet radius reached a plateau value ($\sim 2.5 \mu\text{m}$) after ~ 75 min. The growth in droplet size was slower in the case of the sample with $\varphi_M 0.247$. Eventually, after ~ 10 h, the droplet radius attained the same plateau value as in the case of the mixture of $\varphi_M 0.600$. For the sample of $\varphi_M 0.500$, the droplet growth rate was fast over the first 20 min. Subsequently, the droplet radius kept increasing at a much slower rate for 24 hr, without reaching a plateau value (see Figure 2e, squares).

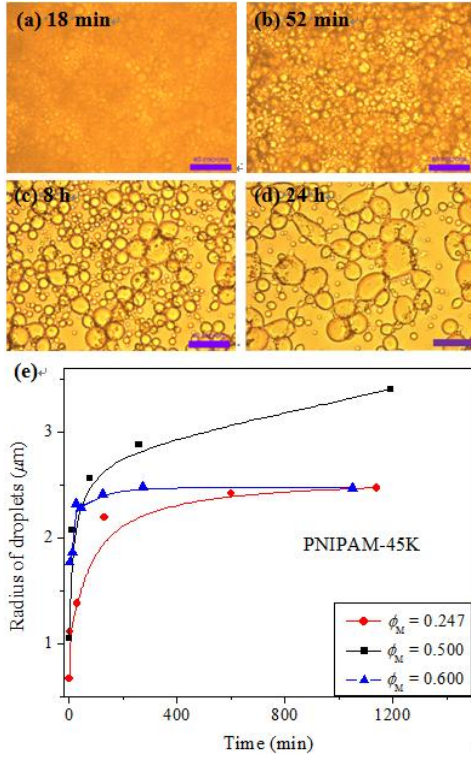


Figure 2. Optical micrographs of PNIPAM-45K/water/methanol mixtures with ϕ_M 0.500 as a function of time following mixing: (a) 18 min, (b) 52 min, (c) 8 h. and (d) 2 days; (Scale bar: 40 μm); (e) Average radius of the dense phase droplets in PNIPAM-45K/water/methanol mixtures as a function of time with $\phi_M = 0.247$, 0.500 and 0.600.

Specimens were observed again 2 days after mixing, which corresponds to the incubation time of the samples used to determine the MLLPS phase boundaries (Figure 1a). The shape and size of the dense phase droplets varied considerably depending on the initial mixture composition, as seen in Figure 3 where we show micrographs recorded for mixtures of $\phi_M = 0.200$, 0.247, 0.500 and 0.600. Mixtures of the lowest initial methanol content ($\phi_M = 0.200$) consist of a network of inter-connected necklaces of small droplets with diameters of $\sim 1 \mu\text{m}$ (see inset in Figure 3a). Although, droplets are observed by microscopy, macroscopically,

.the sample of $\varphi_M = 0.200$ is homogeneous. The specimen with $\varphi_M = 0.247$ contains a network of much larger droplets that vary in size from 2 to 25 μm (Figure 3b). The micrograph of the sample of $\varphi_M = 0.500$ (Figure 3c) presents mostly large areas of the dense phase. They present protrusions linked to small droplets suggesting a gradual coalescence of smaller droplets formed initially in this mixture. The droplets formed in the methanol-rich sample ($\varphi_M = 0.600$) are mostly round in shape (Figure 3d). Their diameters range from 4 to 30 μm . The composition of this sample is the same as the macroscopic sample of lowest cloud point temperature recorded by turbidimetry for mixed systems with a PNIPAM concentration of $1.0 \text{ g} \cdot \text{L}^{-1}$.

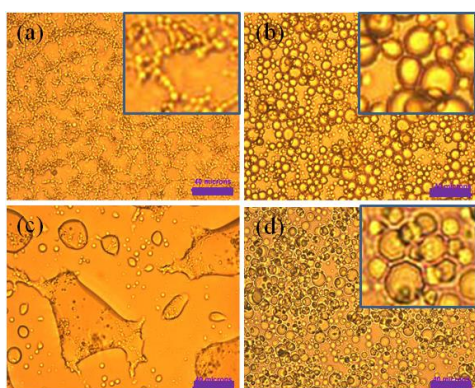


Figure 3. Optical micrographs of PNIPAM-45K/water/methanol mixtures with $\varphi_M =$ (a) 0.200, (b) 0.247, (c) 0.500, and (d) 0.600 after incubation at 21 °C for 2 days (Scale bar: 40 μm). The samples were sealed between two glass slips immediately after mixing. The insets in image (a), (b) and (d) present a 4.5 times enlargement of the corresponding pattern.

There is one common feature amongn the droplets observed in Figures 2 and 3: they are surrounded by a thick high-contrast layer, which we take as an indication that an a large fraction of the polymer concentrates on the rim of the droplets. PNIPAM, which has a higher

refractive index (1.47)³² than either water (1.330) or methanol (1.328), can give rise to differences in contrast within the micrographs in areas of high polymer concentration. To confirm this hypothesis, we observed by fluorescence microscopy the demixion of PNIPAM-45K spiked with a small fraction of pyrene-labeled PNIPAM. A micrograph of the demixed system is shown in Figure 4. The droplets are fluorescent whereas the surrounding lean phase is dark, confirming that the polymer is mostly confined within the dense droplets. A closer look at individual droplets (see inset in Figure 4) reveals that the emission from the rim of the droplets is enhanced significantly, compared to the inner area, which confirms that the polymer resides preferentially on the interface between the lean and dense phases. On the macroscopic level (Figure 1) we observed that the separated liquid phases do not become transparent even after extended time periods. The opacity of the liquids can be attributed to fluctuations of the refractive index within the **sample**, which suggests inhomogeneous/non-uniform distribution of the polymer within the liquid. The opacity may indicate presence of polymeric particles in both phases. Unfortunately, we have not found an experimental possibility to investigate separated phases further.

Figure 4. Micrographs of a PNIPAM-45K/PNIPAM-Py(95.0:5.0 w:w)/methanol/water mixture with $\phi_M = 0.300$ recorded 5 h after mixing; total polymer concentration: 10.0 g L^{-1} ; (a) bright field; (b) fluorescence; $\lambda_{em} = 461 \text{ nm}$; the enlarged droplet in the inset exhibits a strongly fluorescence rim.

The stability of the droplets is related mainly to two factors, the rate of collision between two droplets, of characteristic time τ_c , and the viscoelasticity of the droplets.²⁸ In his studies of demixed polymer solutions, H. Tanaka introduced the characteristic rheological time of polymer-rich droplets, defined as $\tau_t \sim \eta_s b^3 N^3 \Phi^\alpha / k_B T$, where η_s is the solvent viscosity, b is a constant, N is the number of repeating units, Φ is the volume fraction of droplets, and α is the growing exponent. When $\tau_t > \tau_c$, droplets behave as elastic bodies: they collide but do not merge. This mechanism accounts for the stability of turbid PNIPAM/water/methanol

Commented [AV11]: , which suggests inhomogeneous/non-uniform distribution of polymer within liquid. The opacity may indicate presence of polymeric particles in both phases. Unfortunately, we have not found an experimental possibility to investigate separated phases further.

Commented [AV12]: Figure 4 is missing

mixtures against MLLPS of samples of low polymer concentration. When $\tau_t < \tau_c$, droplets coalesce upon collision via the Brownian-coagulation mechanism, analogous to phase-separated binary liquid mixtures.²⁹ Increasing the polymer concentration of the initial mixtures raises the viscosity of the whole system. Thus, the τ_c and the density of the liquid droplets formed upon mixing increases. These factors, together with the fact that methanol may act as a plasticizer for PNIPAM, favour the coalescence of droplets for more concentrated systems.³⁰ The MLLPS of high molar mass PNIPAM is expected to happen only under deep-quench conditions, i.e. only in a narrower composition region. This is already the case for a PNIPAM-80K, for which MLLPS was only observed in mixtures of methanol volume fraction between 0.570 and 0.650 (x_m 0.371 and 0.453), as shown in **Figure S3**.

In this last section, we report how changes in temperature affect PNIPAM-45K/water/methanol samples of ϕ_M 0.140, 0.200, 0.450, and 0.620 prepared at 21°C and kept at this temperature for two days. Figure 5 (a and b) displays photographs of samples heated from 21°C to 45 °C. The mixture of $\phi_M = 0.140$ is a transparent, homogenous solution at 21 °C (Figure 5a). It becomes slightly turbid at 25.5 °C. The turbidity intensifies as the sample temperature reaches 45.5 °C. The sample was incubated at 45.5 °C for 40 hr, after which time a turbid droplet (circled in red in Figure 5a) appeared on the bottom of the vial. The upper layer was slightly less turbid, indicating transfer of polymer from the upper layer to the droplet. The sample of $\phi_M = 0.200$, which is slightly turbid at 21 °C, undergoes MLLPS upon incubation at 24.6 °C for 2 h. The dense phase forms a thin film on the bottom of the flask. Its appearance does not change upon further increase of temperature (Figure S3). The sample with $\phi_M = 0.450$ is phase-separated at 21 °C (Figure 5b). Upon heating past 25.5 °C, the dense phase becomes turbid and the curvature of the droplet increases (Figure 5b). The sample appearance does not change upon incubation at 45.5 °C for 40 h.. After this treatment,

the sample is brought back to 21 °C, whereby the droplet spreads somewhat and clarifies slightly. The sample of $\phi_M = 0.620$ is transparent and homogeneous at 21 °C. It separates in two liquid phases at ~ 29 °C (± 2.5 °C) (Figure S5). For this sample, it was very difficult to measure a cloud point temperature, since the turbidity region is extremely narrow. 1

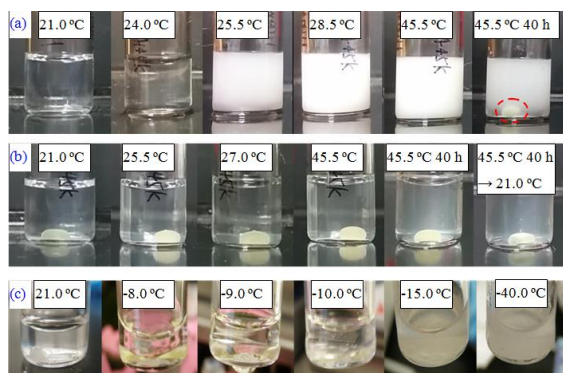


Figure 5. Photographs of PNIPAM-45K/water/methanol mixtures subjected to various treatments: (a) ϕ_M : 0.140, heated stepwise and incubated at each step for 2 h. The solution became cloudy when the temperature reached 24.0 °C.; after incubation at 45 °C for 40 h, a turbid droplet formed on the bottom of the vial (circled in red) (b) ϕ_M : 0.450, heated stepwise and incubated at each step for 2 h. The lean phase became cloudy when the temperature reached 25.5 °C; no further changes occurred upon further heating; upon cooling to 21 °C, the sample recovered to its original appearance. The curvature of the droplet increased with temperature; (c) ϕ_M : 0.450, cooled stepwise and incubated at each temperature for 1 h; it became turbid as the temperature reached -10 °C.

The effect of lowering the temperature below 21 °C was monitored for samples of $0.25 < \phi_M < 0.50$. The sample of ϕ_M 0.346, which is phase-separated at 21 °C, forms a single turbid fluid at 7 °C and becomes transparent below -10 °C. When samples of ϕ_M 0.25 and 0.30 are cooled below ~ 10 °C, they are converted to a single transparent over a narrow temperature range. The change in appearance is extremely abrupt. Mixtures with ϕ_M 0.450 and 0.500, which form two liquid phases at 21 °C, become turbid as they reach -10 °C and -30 °C, they do not become clear down to -40 °C, the freezing temperature of mixed MeOH/water

solutions of $\varphi_M = 0.45$. (Figure 5c). On the basis of the visual observations reported above, we drew the phase diagram of the PNIPAM-45K/MeOH/water system shown in Figure 6. The MLLPS region is bordered by two turbid domains, presumably consisting of stable droplets that resist coalescence. The turbidity region around $\varphi_M \sim 0.60$ is narrow. It was observed when upon heating samples beyond 21 °C, but it was difficult to capture in samples upon cooled below 21 °C. The dashed horizontal line corresponds to $T = 21$ °C.

Figure 6. Phase diagram of PNIPAM-45K/MeOH/water (polymer concentration : 10.0 g L⁻¹); areas shaded diagonally in green correspond to turbid regions; the area shaded horizontally in blue corresponds to the region where MeOH mixtures are frozen (from Haynes, W. M. ; Ed.. CRC Handbook of Chemistry and Physics. 97th ed. ; CRC Press: Boca Raton, FL, 2016; section 5, p 125).

CONCLUSION

The occurrence of MLLPS of PNIPAM/water/methanol mixtures follows patterns similar to the clouding of dilute solutions: for a given polymer sample, it depends on the solvent composition and the temperature. In all cases, the dense phase is both polymer-rich and water-rich, relatively to the original compositions. The MLLPS processes of PNIPAM/water/methanol mixtures monitored by optical microscopy exhibit different kinetics and patterns depending on the compositions of the mixtures. Our study demonstrates that the occurrence of MLLPS is affected by the polymer polar mass and the structure of the end groups, as reflected also in the stability of droplets. Further studies are necessary to understand the role of the end-group hydrophilicity.

ASSOCIATED CONTENT

Supporting Information.

This material is available free of charge via the Internet at <http://pubs.acs.org>.”

Phase diagrams of PNIPAM-45K water/methanol mixtures at $1.0 \text{ g}\cdot\text{L}^{-1}$

Optical photographs of the PNIPAM-45K water/methanol mixtures at $10.0 \text{ g}\cdot\text{L}^{-1}$ with different methanol compositions as a function of temperature,

Composition measurement data,

Optical micrographs of PNIPAM-80K water/methanol mixtures at $10.0 \text{ g}\cdot\text{L}^{-1}$.

AUTHOR INFORMATION

Corresponding Author

* E-mail: francoise.winnik@umontreal.ca

Notes

The authors declare no competing financial interest.

ACKNOWLEDGMENT

The authors are grateful to Professor Fumihiko Tanaka and Dr. Xue-Wei Zhang for many helpful discussions and suggestions. The work was supported by a Discovery grant of F. M. W. from the Natural Sciences and Engineering Research Council of Canada. N. X. was supported by a scholarship from China Scholarship Council.

REFERENCES

For Table of Contents use only.

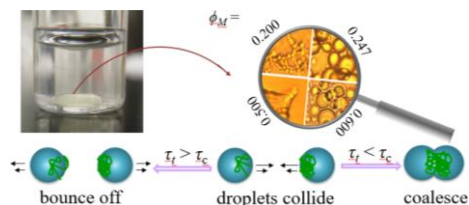
Liquid-Liquid Phase Separation of poly(N-isopropylacrylamide) in Water/Methanol Mixtures

Na Xue[†], Xing-Ping Qiu[†], and Françoise M. Winnik^{*,†,‡,⊥}

[†]Department of Chemistry, University of Montreal, CP6128 Succursale Centre Ville,
Montreal QC Canada H3C 3J7

[‡]World Premier International (WPI) Research Center Initiative, International Center for
Materials Nanoarchitectonics (MANA) and National Institute for Materials Science (NIMS),
1-1 Namiki, Tsukuba 305-0044, Japan

[⊥]Department of Chemistry and Faculty of Pharmacy, University of Helsinki, FI-00014
Helsinki, Finland



1. Halperin, A.; Kröger, M.; Winnik, F. M. *Angewandte Chemie International Edition* **2015**, 54, 15342-67.
2. Winnik, F. M.; Ringsdorf, H.; Venzmer, J. *Macromolecules* **1990**, 23, 2415-6.
3. H.G, S. *Progress in Polymer Science* **1992**, 17, 163-249.
4. Scherzinger, C.; Balaceanu, A.; Hofmann, C. H.; Schwarz, A.; Leonhard, K.; Pich, A.; Richtering, W. *Polymer* **2015**, 62, 50-9.
5. Schild, H. G.; Muthukumar, M.; Tirrell, D. A. *Macromolecules* **1991**, 24, 948-52.
6. Dudowicz, J.; Freed, K. F.; Douglas, J. F. *The Journal of Chemical Physics* **2015**, 143, 131101.
7. Tanaka, F.; Koga, T.; Winnik, F. *Physical Review Letters* **2008**, 101.
8. Zhang, G.; Wu, C. *Journal of the American Chemical Society* **2001**, 123, 1376-80.
9. Mukherji, D.; Marques, C. M.; Kremer, K. *Nat Commun* **2014**, 5, 4882.
10. Rodríguez-Ropero, F.; Hajari, T.; van der Vegt, N. F. A. *The Journal of Physical Chemistry B* **2015**, 119, 15780-8.
11. Pica, A.; Graziano, G. **2016**, 18, 25601-8.
12. Walter, J.; Sehart, J.; Vrabec, J.; Hasse, H. *The Journal of Physical Chemistry B* **2012**, 116, 5251-9.

13. Qiu, X.; Koga, T.; Tanaka, F.; Winnik, F. *Sci. China Chem.* **2013**, 56, 56-64.
14. Tu, C.-W.; Kuo, S.-W. *Journal of Polymer Research* **2014**, 21, 1-8.
15. Yamauchi, H.; Maeda, Y. *The Journal of Physical Chemistry B* **2007**, 111, 12964-8.
16. Hofmann, C. H.; Plamper, F. A.; Scherzinger, C.; Hietala, S.; Richtering, W. *Macromolecules* **2013**, 46, 523-32.
17. Yang, C.; Li, W.; Wu, C. *The Journal of Physical Chemistry B* **2004**, 108, 11866-70.
18. Mukherji, D.; Marques, C. M.; Stuehn, T.; Kremer, K. *The Journal of Chemical Physics* **2015**, 142, 114903.
19. Hore, M. J. A.; Hammouda, B.; Li, Y.; Cheng, H. *Macromolecules (Washington, DC, U. S.)* **2013**, 46, 7894-901.
20. Chee, C. K.; Hunt, B. J.; Rimmer, S.; Soutar, I.; Swanson, L. *Soft Matter* **2011**, 7, 1176-84.
21. Wang, F.; Shi, Y.; Luo, S.; Chen, Y.; Zhao, J. *Macromolecules* **2012**, 45, 9196-204.
22. Tao, C.-T.; Young, T.-H. *Polymer* **2005**, 46, 10077-84.
23. Winnik, F. M. *Macromolecules* **1990**, 23, 233-42.
24. Yip, J.; Duhamel, J.; Qiu, X. P.; Winnik, F. M. *Macromolecules* **2011**, 44, 5363-72.
25. Lee, H.; Hong, W. H.; Kim, H. *Journal of Chemical & Engineering Data* **1990**, 35, 371-3.
26. Katsumoto, Y.; Tsuchiizu, A.; Qiu, X.; Winnik, F. M. *Macromolecules* **2012**, 45, 3531-41.
27. Tanaka, F.; Koga, T.; Kojima, H.; Xue, N.; Winnik, F. o. M. *Macromolecules* **2011**, 44, 2978-89.
28. Hajime, T. *Journal of Physics: Condensed Matter* **2000**, 12, R207.
29. Gunton, J.; San Miguel, M.; Sahni, P. S.; Domb, C.; Lebowitz, J., Phase transitions and critical phenomena. Academic, New York: 1983.

30. Tanaka, H. *The Journal of Chemical Physics* **1996**, 105, 10099-114.
31. Roy, S.; Das, S. K. *Soft Matter* **2013**, 9, 4178-87.
32. Kumaran, V. *The Journal of Chemical Physics* **2000**, 112, 10984-91.
33. Spěváček, J. i.; Hanyková, L.; Labuta, J. *Macromolecules* **2011**, 44, 2149-53.